

# Investigations of the Spectral Characteristics of 980-nm InGaAs–GaAs–AlGaAs Lasers

Ivan A. Avrutsky, Reuven Gordon, R. Clayton, and Jimmy M. Xu, *Senior Member, IEEE*

**Abstract**—Semiconductor quantum-well (QW) lasers at 980 nm exhibit unique spontaneous emission spectra with a periodic envelope of approximately 2~3-nm wavelength. This phenomenon has been observed in both front facet and side spontaneous emission. The modulation is modeled in terms of coupling between the laser waveguide and the substrate waveguide which is transparent to 980-nm light. Modal gain spectra of the entire waveguide structure including substrate are calculated numerically by a transfer matrix method. The gain spectra in the active stripe and loss spectra in the unpumped QW exhibit modulation. This results in modulation of the emission spectra. An analytical approach based on coupled mode equations is developed to explain and clarify the results of the numerical modeling. The interesting case of a coupling length that is small by comparison with the gain/loss length is examined in detail. Front facet and side spontaneous emission spectra calculated using the modal gain spectra are in good agreement with the measured spectra. The results presented make it possible to interpret the unique modal characteristics of 980-nm lasers quantitatively and relate them to the physical structural parameters.

**Index Terms**— Coupled mode analysis, quantum-well lasers, semiconductor waveguides, spontaneous emission.

## I. INTRODUCTION

HIGH-POWER single-mode semiconductor lasers emitting in the 980-nm region attract much attention as a source for pumping of Er-doped optical fiber amplifiers (see, for example, [1], [2] and references therein). The high-power and high-efficiency requirements for laser diodes of this type are being met with much research effort. A shift in attention to the spectral behavior of these devices is expected as a result of the need to reduce mode hopping and improve spectrum stability with both current and temperature changes. In recent experiments, we observed that the spectral characteristics of 980-nm Fabry–Perot lasers show some unique and interesting features in front facet emission below and near lasing threshold, and in the side spontaneous emission for all operating conditions.

One prominent feature is a periodic spectral modulation. Intrigued by the observation of nearly periodic mode hopping in the lasing wavelength, we examined the spectral details

Manuscript received October 25, 1996; revised July 1, 1997. This work was supported by Nortel, OCMR, and NSERC.

I. A. Avrutsky is with the Optoelectronics Laboratory, Electrical and Computer Engineering Department, University of Toronto, Toronto, Ont., Canada M5S 3G4. He is also with the Fiber Optics Research Center, General Physics Institute, Russian Academy of Sciences, Moscow, Russia 117942.

R. Gordon and J. M. Xu are with the Optoelectronics Laboratory, Electrical and Computer Engineering Department, University of Toronto, Toronto, Ont., Canada M5S 3G4.

R. Clayton is with Advanced Technology Labs, Nortel Technology, Ottawa, Ont., Canada K1Y 4H7.

Publisher Item Identifier S 0018-9197(97)07078-4.

of the front facet emission and found periodic modulation superimposed upon the longitudinal cavity's Fabry–Perot oscillations. This observation led us to the investigation of side spontaneous emission which exhibited similar spectral modulation. Furthermore, we found that the period and location of the modulation were invariant to changes in temperature and current. The modulation suggests an additional feedback mechanism at play, and the prospect of controlled mode discrimination if it can be understood and modeled, and thereby engineered. Analysis was done to determine whether the modulation was intrinsic to these lasers and to quantify the feedback mechanism that produces it.

Spectral modulation in the spontaneous emission of a laser has been observed previously. In [3], the authors suggested two possible explanations for the phenomenon: recombination of electrons and holes from different quantized levels and a resonant self-effect of Fabry–Perot cavity modes field via the volume of laser crystal. They confirm the latter model experimentally. Having considered a few different types of closed volume trajectories, they estimated possible modulation periods using geometrical consideration only. The trajectory lying directly under stripe was proven to result in modulation period close to the one observed. It agrees with the emission of light from the substrate under the active stripe.

In [4], an analytical approach was developed to explain the modulation. The authors calculated perturbations to the laser gain spectrum caused by light penetration into the substrate and its reflection from the bottom substrate interface. Their approach is based on a careful analysis of the Helmholtz equation and boundary conditions. However, this approach has the usual shortcoming of obscuring the features and behavior that may lead to more insightful or intuitive understanding of the system. In addition, the approach taken there has necessitated a number of approximations, which apparently has limited its validity to one of the two possible domains, namely crossing (or weak coupling) domain of dispersion curves. Another drawback of the theory is evident in the assumption of lossless light propagation in the substrate and total reflection from the lower substrate boundary, which would result in an infinitely large gain modulation amplitude.

Comprehensive numerical analysis of mode coupling in semiconductor lasers with transparent substrate is made in [5]. The entire laser structure, including the substrate, is treated as a multimode waveguide and the complex propagation constants of the modes are calculated. The authors investigated the laser mode gain spectra for cladding layers and substrates of varying thickness while using wavelength independent material parameters (including the active layer material gain) for the laser layers.

Recent observations of room-temperature In-GaN-GaN-AlGaN multi-quantum-well (MQW) lasers with a substrate that is transparent to the emitted light showed similar modulation patterns to the ones observed here [6]. Although the authors stated that they have not found a proper explanation for the measured spectra modulation, we believe the modulation is caused by the same type of feedback mechanism with a modulation period of about a factor of 6–8 less than those reported here. This reduction in period can be attributed to the laser's operation in the 405–410-nm range and that the modulation period has a quadratic wavelength dependence [4]. These observations imply a broader applicability of the analysis presented here to a similar phenomenon in other laser types.

In this paper, we use a numerical approach analogous to that of [5] to calculate the modal gain. We take into account the spectral dependence of material parameters and calculate not only the gain spectrum but also the spontaneous emission spectrum. The gain modulation was found to depend not only on the thickness and refractive index of the layers but also on the waveguide gain/loss difference between the laser waveguide layer and the substrate. We extended our model to analyze side spontaneous emission by considering light emission in the pumped portion of the waveguide, its propagation along the highly lossy unpumped laser waveguide and coupling to the substrate.

In order to gain insight into and clarify the results of the numerical modeling, we develop a phenomenological analytical approach based on coupled mode theory. The coupling constant used in this approach is determined by a well-established numerical formulation. Nevertheless, the phenomenological approach provides a general and clear description of the coupling induced modal gain modulation.

The gain spectrum modulation period is determined by phase matching between the high gain laser waveguide and substrate waveguide with losses. An analogous loss spectrum modulation takes place for the case of the side waveguide laterally adjacent to the laser ridge. This model relates the gain/loss modulation to the waveguide parameters and can thereby facilitate future design efforts taking advantage of these phenomena.

## II. EXPERIMENTAL RESULTS

The lasers under investigation were fabricated by metal-organic chemical vapor deposition. The details of the laser structure are listed in Table I and the schematic view of the laser is shown in Fig. 1. Front and rear laser facets were coated to receive 10% and 90% reflectivity, respectively. The lasers were mounted “p-side up,” so an increase in the laser temperature is expected with an increase of pumping current even with a stabilized heat sink temperature. On the other hand, it allowed us to easily collect the spontaneously emitted light both from the front facet and from the side facet by using a tapered fiber. As will be shown in the calculations, the spectral modulation of the laser waveguide emission originates in the coupling between the laser waveguide and the transparent substrate. For this reason, if the light collection is not sufficiently focused on the laser waveguide, light coupled

TABLE I  
PARAMETERS OF THE QUANTUM WELL

Parameter	Well	Barrier
Material	In <sub>0.2</sub> Ga <sub>0.8</sub> As	Al <sub>0.1</sub> Ga <sub>0.9</sub> As
Bandgap e-hh	1.2157eV	1.5404eV
Bandgap e-lh	1.2947eV	1.5412eV
Conduction band offset	0.1821eV	
Valance hh band offset	0.1426eV	
Valance lh band offset	0.0644eV	
Electron mass	0.0622	0.076
HH mass	0.358	0.359
LH mass	0.0694	0.0797
Well width	80 Å	-
Minority carrier density	3.6e18 cm <sup>-3</sup>	-
Intraband relaxation time	0.1 ps	

\*Materials are supposed to be strained to match the lattice constant to (100) GaAs substrate.

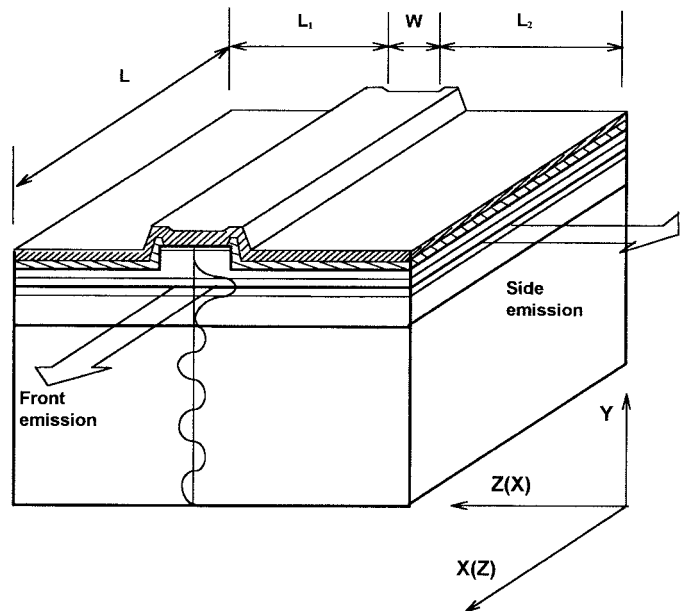


Fig. 1. Schematic view of the laser structure.

to the substrate will also be observed in the spectra and the spectral modulation will be significantly reduced. Spectra taken with the fiber was discriminating enough to clearly show the modulation phenomenon in the laser waveguide emission (which is relevant to laser applications).

The fiber tip was mounted on a two-dimensional piezoelectric moving stage of submicrometer precision with a high precision nanomover along the remaining longitudinal direction. The spectra were recorded by means of an optical spectrum analyzer HP70951A. The same technique was successfully used previously for longitudinal carrier density profiling in semiconductor lasers via spectral analysis of side spontaneous emission [7].

Several steps were taken to ensure that the spectral modulation obtained was truly characteristic of the laser waveguide emission.<sup>1</sup> White light emission from a halogen lamp was coupled into the fiber and showed no spectral modulation in the wavelength range of our laser observations. The distance between the fiber tip and the facet was varied over the range of 1 cm to ensure that the modulation phenomenon did not result from external cavities in the setup. Both cleaved and tapered

<sup>1</sup>The constructive critique of the reviewer is credited.

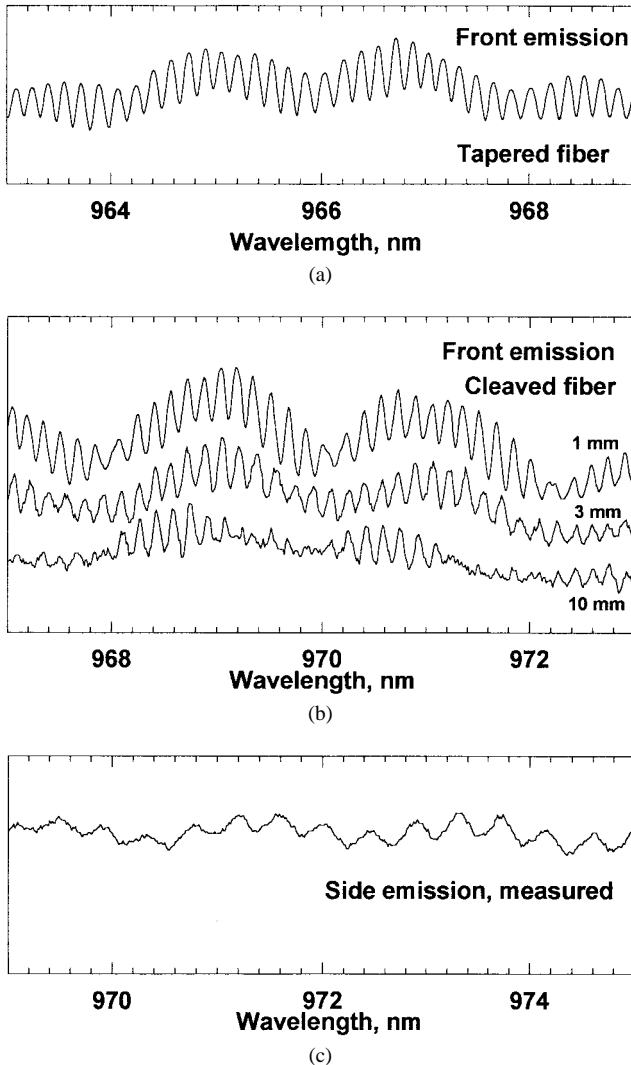


Fig. 2. The measured spontaneous emission spectra from (a) the front facet for a tapered fiber, (b) a cleaved fiber at three different fiber tip-facet distances and (c) from the side facet.

fibers were used to observe the spectral modulation in the laser emission to preclude modulation from the fiber tip structure. The modulation was observed consistently for several lasers with the same structure as described above.

Typical features of the front facet spontaneous emission are shown in Fig. 2(a) and (b) for light emission collected by tapered and cleaved fibers at several fiber tip-facet displacements. Clearly resolved Fabry-Perot oscillations corresponding to the resonator length are modulated by an envelope periodic function with a period of about 2 nm. The slow modulation amplitude was found to increase as the pumping current approaches threshold. There is also a baseline envelope of the same period. It is important to note that the spectrum analyzer resolution (0.1 nm) was half the period of the Fabry-Perot oscillations. This is probably the cause of the observed baseline envelope, as is accounted for and shown in the modeling.

Side facet spontaneous emission spectra were recorded at pumping currents below and above the threshold current [an example of the spectrum is shown in Fig. 2(c)]. These side spectra contain fast oscillations with a period corresponding to

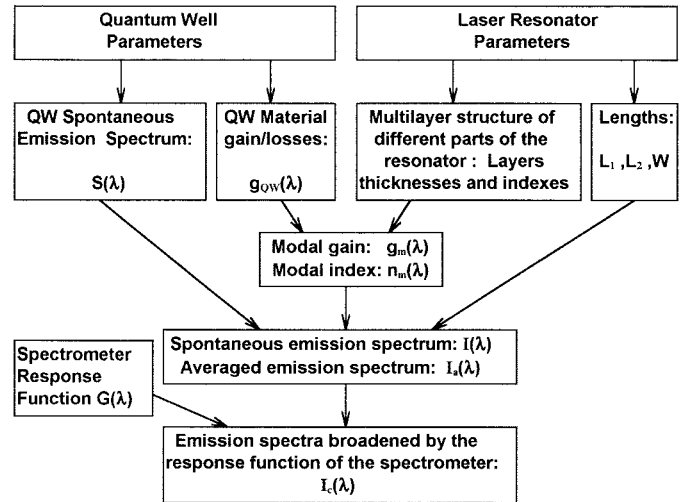


Fig. 3. The scheme for modeling the spontaneous emission spectra.

the lateral width of the laser structure and slow modulation of approximately 2 nm analogous to those of the front emission spectra. We studied lasers with different cleaving distances between the laser stripe and the side facet and found that the magnitude of the slow modulation relative to the background increases as this distance increases, but not the period.

The spontaneous emission spectra were investigated at different heatsink temperatures, in CW and pulse regimes with duty cycles from 20% to 80%. The spectral positions of maximums and minimums of the slow modulation were found to be independent of the temperature and current change while the positions of Fabry-Perot oscillations and general spectrum envelope were temperature- and current-dependent. This observation offers the opportunity for laser output wavelength stabilization and emphasizes the importance of accurate modeling of the phenomenon.

### III. THEORY

#### A. Modal Gain in Coupled Waveguides: Simulation by the Transfer Matrix Method

The observed slow modulation in spontaneous emission spectra implies an additional feedback mechanism in the laser. Looking for this mechanism, we analyzed the typical structure of the 980-nm fiber pump laser. Such a laser contains a QW InGaAs as an active region waveguide layer made of GaAs, GRIN AlGaAs or GRIN InGaAsP, cladding layers of AlGaAs or InGaP, and a GaAs substrate. It is a peculiarity of lasers emitting in the wavelength region of 980 nm that they have a substrate transparent to the emission wavelength with a refractive index just above the effective refractive index of the laser waveguide. So, the substrate itself is a very thick waveguide which can be coupled to the laser waveguide due to light tunneling through the cladding layer.

The modal gain and the modal index of the entire multilayer waveguide structure, including the substrate, were calculated by means of a transfer matrix method. The modeling scheme is presented in Fig. 3. We used the layer parameters listed in Table I. The QW material gain  $g_{QW}(\lambda)$  and the spontaneous emission spectrum of the QW itself were calculated by the

## QW material parameters

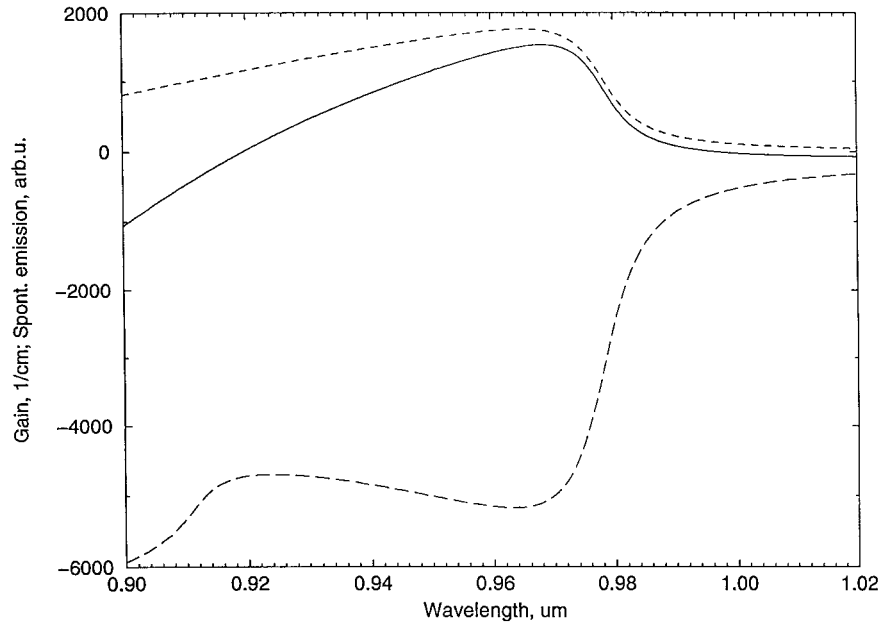


Fig. 4. The modeled quantum well gain (solid line), loss (long dashed line) and spontaneous emission (short dashed line) spectra.

TABLE II  
WAVEGUIDE LAYER PARAMETERS USED FOR MODE GAIN AND  
MODE INDEX CALCULATED BY THE MATRIX TRANSFORM METHOD

Layer name	Material	Refractive index	Absorption index	Thickness, $\mu\text{m}$ stripe region / etched region
Top metal	Au	0.24	6.5	$\infty / -$
Dielectric	$\text{SiO}_2$	1.46	0.0	$0 / \infty$
Contact layer	p-GaAs	$n(\lambda, x=0.0)^{**}$	$30[\text{cm}^{-1}]:\lambda/4\pi$	$0.1 / 0.0$
Top Clad	$\text{Al}_{0.3}\text{Ga}_{0.7}\text{As}$	$n(\lambda, x=0.3)^{**}$	$10[\text{cm}^{-1}]:\lambda/4\pi$	$2.0 / 0.2$
Top GRIN	$\text{Al}_x\text{Ga}_{1-x}\text{As}$ , $x=0.3 \rightarrow 0.1$	$n(\lambda, x)^{**}$ , $x=0.3 \rightarrow 0.1$	$10[\text{cm}^{-1}]:\lambda/4\pi$	Ten layers of constant index and equal thickness $10 \times 0.011$
QW	$\text{In}_{0.2}\text{Ga}_{0.8}\text{As}$	3.6	$-g_{\text{QW}}(\lambda):\lambda/4\pi$	0.008
Bottom GRIN	$\text{Al}_x\text{Ga}_{1-x}\text{As}$ , $x=0.1 \rightarrow 0.3$	$n(\lambda, x)^{**}$ , $x=0.1 \rightarrow 0.3$	$10[\text{cm}^{-1}]:\lambda/4\pi$	Ten layers of constant index and equal thickness $10 \times 0.011$
Bottom Clad	$\text{Al}_{0.3}\text{Ga}_{0.7}\text{As}$	$n(\lambda, x=0.3)^{**}$	$10[\text{cm}^{-1}]:\lambda/4\pi$	2.0
Substrate	GaAs	$n(\lambda, x=0.0)^{**}$	$30[\text{cm}^{-1}]:\lambda/4\pi$	110.0
Bottom metal	Au	0.24	6.5	$\infty$

\*Material gain spectrum in QW layer was calculated by the algorithm described in [6].

\*\*Refractive index of  $\text{Al}_x\text{Ga}_{1-x}\text{As}$  was calculated by the Sellmeier formula:  $n(\lambda, x) = [A(x) + B(x)/(\lambda^2 - C(x)) - D(x)\lambda^2]^{1/2}$ , where  $A(x) = 13.5 - 15.4x + 11.0x^2$ ,  $B(x) = 0.690 + 3.60x - 4.240x^2$ ,  $C(x) = 0.154 - 0.476x + 7.00x^2$ , and  $D(x) = 1.84 - 8.18x + 7.00x^2$ .

approach described in [8] and are illustrated in Fig. 4. Energy band parameters used in the modeling are shown in Table II. From these, the modal gain spectrum was obtained (as shown in Fig. 5). Fig. 5 also shows the modal gain with an infinitely thick cladding layer to illustrate the influence of the substrate upon the noncoupled modal gain. The laser spontaneous emission spectra from the front and side facets were calculated using the formulae given in Section III-C of this paper. The modal gain spectrum modulation with a period of approximately 2 nm and modulation depth of  $0.5 \sim 1 \text{ cm}^{-1}$  results in a strong modulation of spontaneous emission spectra from the front facet at a current just below threshold.

Our model is based on a one-dimensional (1-D) analysis. To account for the lateral divergence of the radiation which

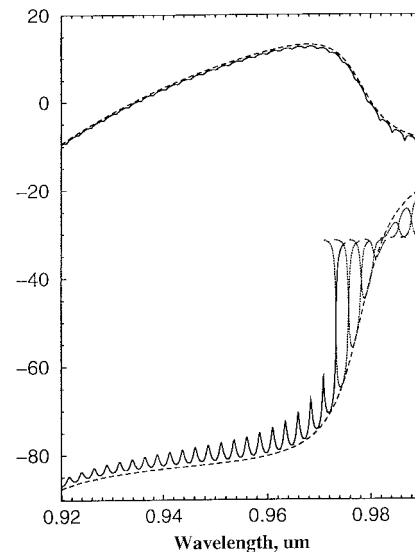


Fig. 5. The calculated gain spectrum with coupling (solid line) and without coupling (infinitely thick cladding layer: dashed line). The curves in the positive gain region are calculated for the laser stripe at carrier concentration of  $0.9 \times$  threshold. The curves in the negative gain region correspond to the waveguide beyond the laser ridge, with the carrier concentration approaching zero. The dotted lines represent gain (loss) spectra when anticrossing in the dispersion characteristics takes place.

tunnels into the substrate, an additional absorption factor is included in the substrate layer.

In modeling the side emission spectra, we assumed that spontaneous light is emitted in the region under the laser stripe and that it propagates through the unpumped portion of the waveguide. Light in the unpumped region of the QW layer experiences high optical losses. The modal loss spectrum is also wavelength modulated due to coupling between this portion of the waveguide and the substrate (Fig. 5). The loss

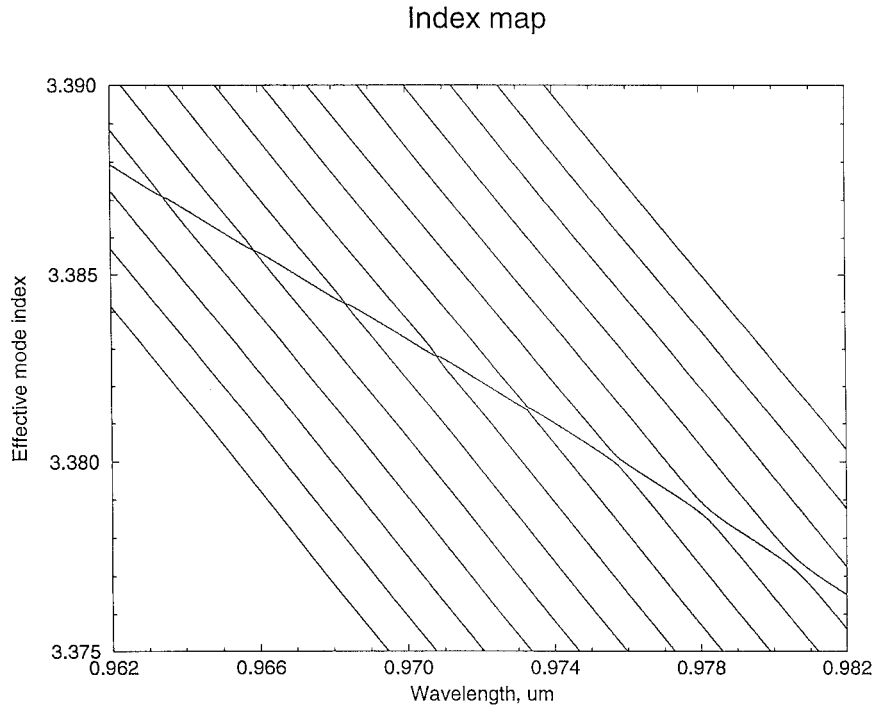


Fig. 6. Modal index map for the entire laser structure including the substrate.

modulation results in a corresponding side facet emission spectra modulation. It is worth while noting that to achieve a large modulation of the side emission spectrum the modal loss modulation should be much larger than the value of the modal gain modulation. The reason for such a difference in spontaneous emission from the front and side facet will become clear with the analysis of a Fabry–Perot resonator with parts of gain and loss. Actually, away from the laser ridge the waveguide coupling with the substrate is stronger because the thinner top cladding layer pushes the waveguide mode down. To achieve reasonable modulation, we modeled the effective thickness of the top cladding layer (accounting for the effect passivation layer) as being  $0.2 \mu\text{m}$ .

The calculated mode dispersion curves of the waveguide are shown in Fig. 6. The array of nearly parallel curves with greater negative slope corresponds to modes localized mostly in the substrate while the curves of smaller negative slope belong to the laser waveguide. The case of an unpumped QW is shown here because it illustrates well the influence of loss on mode coupling. When modal loss (gain) is small in comparison with the coupling constant (for wavelengths  $\lambda > 0.973 \mu\text{m}$  as in Fig. 6), we see the well-known anticrossing behavior. The anticrossing effect is absent when loss (gain) in coupled waveguides is larger than the coupling constant. With this figure, it is easy to see a correlation between the modal loss spectrum and the dispersion curves. When the effective index of the laser waveguide equals that of the substrate waveguide, the coupling between the two waveguides leads to reduced modal losses. In the case of net gain in the laser waveguide, the coupling results in gain suppression in the laser waveguide at resonance wavelengths.

In principle, the results of this model suffice to explain the observed phenomenon. Nevertheless, the numerical analysis

itself does not offer direct insight into the physics of the spontaneous emission spectra modulation and its dependence on the structural parameters. Therefore, in addition to accurate numerical modeling we take an analytical approach.

### B. Coupled Mode Theory for Waveguides with a Gain

In accordance with a standard coupled mode approach, let us consider an electromagnetic field of the laser waveguide mode and one of the substrate modes which is close to resonance with the laser mode in the form

$$E_L(x, y) = E_L^0(y)L(x) \exp(i\beta_L x), \quad \beta_L = \beta'_L + i\beta''_L \quad (1)$$

$$E_S(x, y) = E_S^0(y)S(x) \exp(i\beta_S x), \quad \beta_S = \beta'_S + i\beta''_S. \quad (2)$$

If we denote the mode emission direction as the  $x$  axis, the mode field distributions depend only on  $y$  coordinate and are uniform along the other transverse direction ( $z$ ).

The coupled mode equations for slowly varying amplitudes  $L(x)$  and  $S(x)$  are

$$dL(x)/dx = i\kappa_{LS}S(x) \exp(i(\beta_S - \beta_L)x) \quad (3)$$

$$dS(x)/dx = i\kappa_{SL}L(x) \exp(i(\beta_L - \beta_S)x). \quad (4)$$

They allow us to construct supermodes with a propagation constant

$$\gamma_{L,S} = (\beta_L + \beta_S)/2 \pm (((\beta_L - \beta_S)/2)^2 + K)^{1/2} \quad (5)$$

$$K = \kappa_{LS}\kappa_{SL}. \quad (6)$$

Now we will take into account the specificity of the waveguides under consideration. The laser waveguide itself typically has a gain  $g_L = -2\beta''_L$  of the order of tens of inverse centimeters. The substrate waveguide has a loss  $\alpha_S = 2\beta''_S$  of up to ten inverse centimeters due to bulk and bulk-metal interface absorption. The coupling constant  $|K|^{1/2}$  is typically much less than the difference of the imaginary parts of

propagation constants  $\beta_S'' - \beta_L'' = (\alpha_S + g_L)/2$  because lasers are normally designed to have strong transverse confinement to the gain cavity. So under the condition

$$|K| \ll ((\beta_S'' - \beta_L'')/2)^2 \quad (7)$$

we receive from (5) the propagation constants of the normal cavity mode and substrate-like mode, respectively:

$$\gamma_L = \beta_L + K/(\beta_L - \beta_S); \quad (8)$$

$$\gamma_S = \beta_S - K/(\beta_L - \beta_S). \quad (9)$$

Further simplification to (8) seems to be possible under an additional reasonable assumption

$$\text{Im}(K) \ll \text{Re}(K) \quad (10)$$

and linearization of dispersion curves in the vicinity of wavelength  $\lambda_o$  corresponding to phase-matching condition

$$\beta_L'(\lambda) - \beta_S'(\lambda) = b(\lambda - \lambda_o) \quad (11)$$

$$b = (d\beta_L'/d\lambda)|_{\lambda_o} - (d\beta_S'/d\lambda)|_{\lambda_o}. \quad (12)$$

Substituting (11) and (12) into (8), we receive

$$\gamma_L = \beta_L + K/b$$

Using typical values for a semiconductor laser, it can be shown that  $dn^*/d\lambda \approx dn_c/d\lambda$ . This means that under the assumption (22) the waveguide mode is localized mostly in cladding layers, therefore, details of the actual waveguide structure are not essential to the dispersion relation.

An analogous analysis can be made for the substrate waveguide. A simplified structure with a layer of thickness  $D$  and refractive index  $n_s$  confined by an ideal metal from below and a cladding medium of index  $n_c$  from above facilitate a dispersion relation of the form

$$(2\pi D/\lambda)(n_s^2 - n_c^2)^{1/2} = \arctan((n_s^2 - n_c^2)/(n_s^2 - n_c^2))^{1/2} + (M + 1/2)\pi \quad (25)$$

where  $M$  is a mode number, typically in the hundreds ( $M \approx (2D/\lambda)(n_s^2 - n_c^2)^{1/2}$ ). For analysis of coupling, we are interested only in modes with an effective index close to that of the laser mode. It allows us to use an inequality analogous to (22)

$$(n^* - n_c)/(n_s - n_c) \ll 1 \quad (26)$$

$$n^{*2} = n_s^2 - (M(\lambda/2D))^2 \quad (27)$$

$$dn^*/d\lambda = n^{*-1}(n_s \cdot dn_s/d\lambda - M^2\lambda/4D^2) \approx dn_s/d\lambda - (n_s^2 - n_c^2)/n_c\lambda. \quad (28)$$

The dispersion of the substrate's modal refractive index contains a term equal to the material dispersion of the substrate and a waveguide dispersion term that is independent of the layer thickness and the mode number provided that (26) is satisfied. The effective index difference for adjacent modes according to (27) is equal to  $(n_s^2 - n_c^2)^{1/2}\lambda/2Dn^*$ . This allows us to find the period of modulation

$$\lambda_M - \lambda_{M+1} = \frac{(n_s^2 - n_c^2)^{1/2}(\lambda/2Dn_c)}{dn_c/d\lambda - dn_s/d\lambda + (n_s^2 - n_c^2)/n_c\lambda}. \quad (29)$$

So, the period of the gain modulation is roughly determined by the indices of the substrate  $n_s$  and cladding layer  $n_c$ , their dispersion relations, the substrate thickness  $D$  and the wavelength  $\lambda$ .

To obtain (29) we used (23), (24), (27), and (28) for waveguide effective index dispersion. The accuracy of the estimated period is of the order of the left side of (22) and (26).

### C. Spontaneous Emission Spectrum of the Semiconductor Laser

Let us consider a Fabry–Perot laser resonator with mirror reflection coefficients  $R_1$  and  $R_2$ . As shown in Fig. 1, let us assume regions of length  $L_1$  and  $L_2$  adjacent to the ridge have optical loss  $\alpha(\lambda)$  and the region of width  $W$  has a gain coefficient  $g(\lambda)$ . Let us further assume that the refractive indices of the lossy and gain regions,  $n_g$  and  $n_l$ , are sufficiently close to prevent light reflection between different parts of the resonator. The chosen configuration of the laser resonator will allow us to consider spontaneous emission either from the front facet or from the side facet by just exchanging the axes  $x$  and  $z$ . In the case of front emission,  $L_1 = L_2 = 0$  and  $W$  should be the cavity length. In the case of side emission, we will use

the laser ridge width as a parameter  $W$  and the parameters  $L_1$  and  $L_2$  will be equal to distances from the laser stripe to the side facets.

As aforementioned, a laser structure containing a thick substrate waveguide supports many supermodes. We will only consider the supermode most localized in the laser waveguide. To observe spontaneous emission, the gain is below the threshold gain needed for lasing, thus

$$A = (R_1 R_2)^{1/2} \exp(gW - \alpha(L_1 + L_2)) \leq 1, \quad (30)$$

If each infinitely thin slice of the pumped region of total length  $W$  emits light spontaneously with spectral density  $S(\lambda)$  and the efficiency of spontaneously emitted light coupling into the mode under consideration is  $M(\lambda)$ , total radiation from the first facet will be equal to

$$I \approx S(\lambda)M(\lambda)n(1 - R_1) \frac{(e^{gW} - 1)}{gW} \times \frac{(e^{-\alpha L_1} + R_2 e^{-\alpha(2L_2 + L_1) + gW})}{|1 - (R_1 R_2)^{1/2} e^{-\alpha(L_2 + L_1) + gW + i(4\pi n L/\lambda)}|^2}. \quad (31)$$

Equation (31) is obtained by calculating the output light intensity produced by each slice inside the Fabry–Perot resonator and subsequent integration along the active region of the length  $W$ . In the equation,  $n$  is the average refractive index of the resonator medium  $n = (n_g W + n_l(L_1 + L_2))/L$ , where  $L$  is a total resonator length:  $L = W + L_1 + L_2$ . This is allowed by the assumption laid out at the start of this section. In the case of front facet emission, i.e., at  $L_1 = L_2 = 0$ ,  $L = W$ , the obtained expression for the spontaneous emission spectrum coincide with the analogous one given in [11].

In (31), the term

$$H(\lambda) = \frac{1}{|1 - (R_1 R_2)^{1/2} e^{-\alpha(L_2 + L_1) + gW + i(4\pi n L/\lambda)}|^2} = \frac{1}{1 + A^2 - 2A \cos(4\pi n L/\lambda)} \quad (32)$$

is responsible for the fast oscillation in the spontaneous emission spectrum with wavelength period corresponding to longitudinal modes of the resonator. Its analysis leads to a Hakki–Paoli formula [12] for determination of a gain spectrum from spontaneous emission spectrum

$$g = \frac{-1}{2L} \ln(R_1 R_2) + \frac{1}{L} \ln \frac{I_{\max}^{1/2} - I_{\min}^{1/2}}{I_{\max}^{1/2} + I_{\min}^{1/2}} \quad (33)$$

where

$$I_{\max} = I(\lambda_{\max}); \quad \cos(4\pi n L/\lambda_{\max}) = 1 \\ I_{\min} = I(\lambda_{\min}); \quad \cos(4\pi n L/\lambda_{\min}) = -1. \quad (34)$$

If the longitudinal mode separation  $\Delta\lambda = \lambda^2/2nL$  is small by comparison to the spectrometer's spectral resolution, the measured intensity will be proportional to the averaged function

$$\langle H(\lambda) \rangle = \frac{1}{\Delta\lambda} \int_{\lambda_{\max}(N)}^{\lambda_{\max}(N+1)} H(\lambda) d\lambda = \frac{1}{1 - A^2} = \frac{1}{1 - R_1 R_2 e^{-2\alpha(L_2 + L_1) + 2gW}}. \quad (35)$$

Then, instead of (31), the emission spectrum will be equal to

an averaged one

$$I_a \approx S(\lambda)M(\lambda)n(1 - R_1) \frac{(e^{gW} - 1)}{gW} \times \frac{(e^{-\alpha L_1} + R_2 e^{-\alpha(2L_2 + L_1) + gW})}{1 - R_1 R_2 e^{-\alpha(L_2 + L_1) + 2gW}}. \quad (36)$$

The spontaneous emission spectrum of the active medium  $S(\lambda)$  was calculated by the same approach as used for the calculation of material gain  $g_{QW}(\lambda)$ . To calculate the optical losses in the unpumped side regions of the laser structure, we found the material loss by determining the negative gain as the carrier density approaching zero

$$\alpha_{QW}(\lambda) = -g_{QW}(\lambda)|_{N \rightarrow 0} \quad (37)$$

and then we used the transform matrix algorithm to find the modal loss.

As we have seen in the previous section, the modal gain spectrum may be modulated with a spectral period much larger than longitudinal mode separation but still less than the gain's spectral width for typical laser parameters. This leads to subsequent superimposed modulation of emission spectra.

Finally, to make the comparison with experimental results easier, the emission spectra calculated by the above algorithm were subjected to numerical convolution with a Gaussian function of width  $\Gamma = 0.1$  nm corresponding to spectral resolution of the spectrometer

$$I_c(\lambda) = \int I(\lambda - \mu)G(\mu) d\mu$$

$$G(\mu) = (2/\Gamma)(\ln 2/\pi)^{1/2} \exp(-4 \ln 2(\mu/\Gamma)^2). \quad (38)$$

The modeled spectra are presented in Fig. 7(a) and (b). They were obtained without parameter fine-tuning except for the top cladding layer thickness beyond the laser stripe which was taken to be  $\sim 0.2 \mu\text{m}$ . This change was made to obtain clearly visible modulation of the side emission spectra. The measured front facet emission spectral modulation appears stronger than the modeled one. This may be caused by the plasma-induced negative index change in the pumped waveguide. Such change leads to widening of the laser mode and stronger coupling.

Temperature change is easily incorporated in the above theoretical approach. Increase in temperature was found to result in: 1) a red shift in the QW material gain profile; 2) an increase in refractive index of the laser layers and consequently a red shift in the fast Fabry-Perot oscillations of the spontaneous emission spectrum; and 3) a shift up of all of the dispersion curves (Fig. 6) but the intersection locations of the dispersion curves remaining practically unshifted. Thus, the spectral positions of the modulation peaks in spontaneous emission spectra for given laser structure are stable. This is in agreement with the experimental observations and suggests an opportunity for lasing wavelength selection and stabilization.

#### IV. CONCLUSION

We have presented experimental findings and a detailed theory of periodical modulations in spontaneous emission spectra of 980-nm semiconductor lasers. Both an elaborate numerical approach and analytical expressions suitable for simple estimations are presented. We showed that the investi-

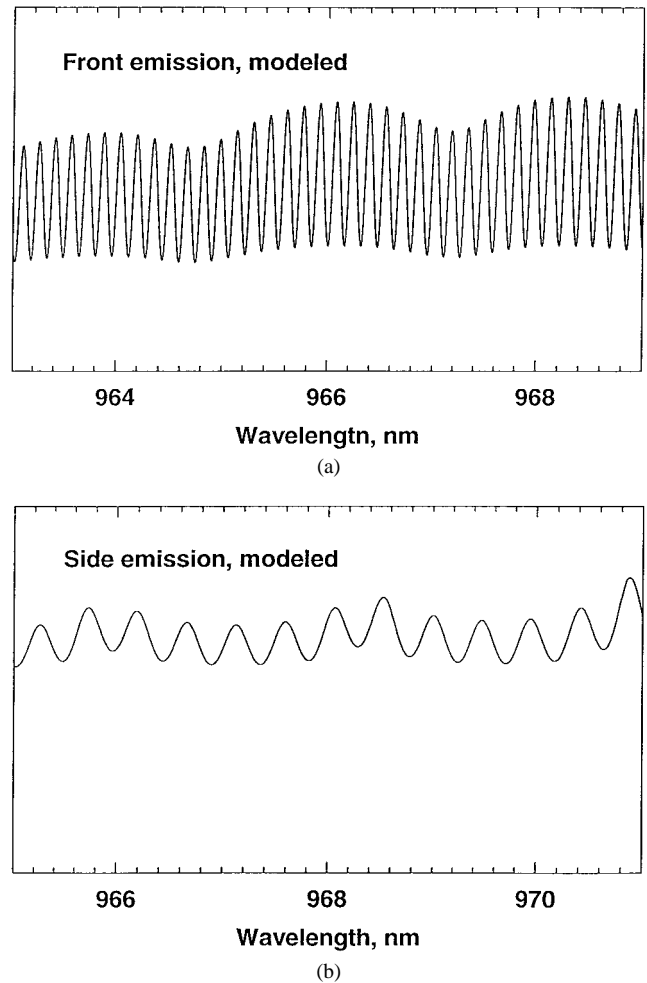


Fig. 7. The modeled spontaneous emission spectra from (a) the front facet and (b) from the side facet.

gated phenomenon is an intrinsic property of 980-nm lasers and should be taken into account in designing them. We attributed the modulation to an additional feedback mechanism that originates from the coupling between the intentionally designed laser cavity and the parasitic substrate waveguide. We find that the coupling involves primarily the very high order substrate modes that are nearly phase matched to the laser guide mode. These high-order modes are in resonance with the lasing mode at nearly equally spaced wavelengths ( $2\sim 3$ -nm spacing for a typical structure). The resonance frequencies are insensitive to temperature or current changes for both the substrate waveguide and the laser guide change in the same way when these parameters are varied. All these key features are in good agreement with the experimental observations.

#### ACKNOWLEDGMENT

The authors thank G. L. Tan for the use of the computer programs STRAIN and GAIN developed by him for the simulation of spontaneous emission and material gain in strained QW structures. They are grateful to all the members of Optoelectronics Laboratory at the University of Toronto for many fruitful discussions, especially to Dr. A. Tager and E. Sargent.

## REFERENCES

- [1] H. Asonen, A. Ovtchinnicov, G. Zhang, J. Nappi, P. Savolaine, and M. Pessa, "Aluminum-free 980-nm GaInAs/GaInAsP/GaInP pump lasers," *IEEE J. Quantum Electron.*, vol. 30, pp. 415–423, 1994.
- [2] N. Chang, S. N. G. Chu, N. K. Dutta, J. Lopata, M. Geva, A. V. Syrbu, A. Z. Mereutsa, and V. P. Yakovlev, "Growth and fabrication of high-performance 980-nm strained InGaAs quantum-well lasers for erbium-doped fiber amplifiers," *IEEE J. Quantum Electron.*, vol. 30, pp. 424–440, 1994.
- [3] E. A. Arjanov, O. V. Danilina, V. P. Konyaev, A. S. Logginov, V. I. Shveikin, and I. I. Vinogradov, "InGaAs strained-layer single-quantum-well lasers spontaneous emission spectra and their features," *Proc. SPIE*, 1994, vol. 2139, pp. 146–153.
- [4] E. A. Arzhanov, A. P. Bogatov, V. P. Konyaev, O. M. Nikitina, and V. I. Shveikin, "Waveguiding properties of heterolasers based on InGaAs/GaAs strained quantum well structures and characterization of their gain spectra," *Quantum Electron.*, vol. 24, pp. 581–587, 1994.
- [5] P. G. Eliseev and A. E. Drakin, "Analysis of the mode internal coupling in InGaAs/GaAs laser diodes," *Laser Phys.*, vol. 4, pp. 485–492, 1994.
- [6] S. Nakamura, M. Senoh, S.-I. Nagahama, N. Iwasa, T. Yamada, T. Matsushita, Y. Sugimoto, and H. Kiyoku, "Room-temperature continuous-wave operation of InGaN multi-quantum-well structure laser diodes with a lifetime of 27 hours," *Appl. Phys. Lett.*, vol. 70, pp. 1417–1419, 1997.
- [7] E. H. Sargent, D. Pavlidis, H. Anis, N. Golinescu, J. M. Xu, R. Clayton, and H. B. Kim, "Longitudinal carrier density profiling in semiconductor lasers via spectral analysis of side spontaneous emission," *J. Appl. Phys.*, vol. 80, pp. 1904–1906, 1996.
- [8] G. Tan, K. Lee, and J. M. Xu, "Finite element light emitter simulator (FELES): A new 2D software design tool for laser devices," *Jpn. J. Appl. Phys.*, vol. 32, pt. 1, pp. 583–589, 1993.
- [9] D. G. Hall, Ed., "Selected paper on coupled mode theory in guided-wave optics," *SPIE Milestones Series*. Bellingham, WA: SPIE, 1993, vol. MS84.
- [10] D. Marcuse, "Dielectric couplers made of nonidentical asymmetric slabs, Part 1: Synchronous couplers," *J. Lightwave Technol.*, vol. LT-5, pp. 178–183, 1987.
- [11] C.-S. Chang, S. L. Chuang, J. R. Minch, W.-C. W. Fang, Y. K. Chen, and T. Tanbum-Ek, "Amplified spontaneous emission spectroscopy in strained quantum-well lasers," *IEEE J. Select. Topics Quantum Electron.*, vol. 1, pp. 1100–1107, 1995.
- [12] B. W. Hakki and T. L. Paoli, "Gain spectra in GaAs double-heterostructure injection lasers," *J. Appl. Phys.*, vol. 46, pp. 1299–1306, 1975.



**Ivan A. Avrutsky** was born in 1963 in the Ukraine. He graduated with honors from the Moscow Physical-Technical Institute in 1986 and received the Ph.D. degree from the General Physics Institute, Russian Academy of Sciences, in 1988.

While at the Moscow Physical-Technical Institute, he was awarded The Kurchatov Stipend and performed postgraduate studies. Since 1983, he has been involved in research carried out at the General Physics Institute of the Russian Academy of Sciences and his responsibility was the experimental study of laser-induced surface gratings on semiconductors and multilayer dielectric structures. From 1983–1991, he worked at the Department of Oscillations, headed by the Nobel Prize winner A. M. Prokhorov, and received a strong background in laser physics. Since 1985, he has worked on an investigation of interference phenomena in a periodically corrugated waveguide. In 1992, he joined the Fiber Optics Research Center, Russian Academy of Sciences, as a Senior Research Fellow. He headed a research group dealing with optical characterization of semiconductor quantum-well structures. He also coordinated a collaborative research project with Nizhny Novgorod Physical-Technical Institute on the development of the technology of aluminum-free quantum-well semiconductor lasers for optical fiber amplifiers. He maintained close contacts with educational institutes like Moscow Physical-Technical Institute and Lomonosov State University, Moscow, supervising students' diploma work (M.Sc. level). Since 1996, he has been at the Optoelectronics Laboratory, University of Toronto, Toronto, Ont., Canada. He is currently interested in optical properties of nanostructured material. He also works on new types of semiconductor lasers like lateral current injection lasers and widely tunable lasers. These projects are sponsored by the Advanced Technology Lab, Nortel Technology.

Dr. Avrutsky received first prize in the competition of young scientists of the General Physics Institute in 1990 for his research on corrugated waveguides, particularly on unidirectional coupling in doubled grating waveguides.



**Reuven Gordon** was born in 1975. He received the B.A.Sc. degree from the University of Toronto, Toronto, Ont., Canada, in 1997. He is currently in their Masters program.

His research to date has focused on high-power 980-nm semiconductor lasers with specific interests in anomalous spectral features and intermodal interaction dynamics.

**R. Clayton**, photograph and biography not available at the time of publication.



**Jimmy M. Xu** (M'87–SM'91) received the Ph.D. degree in electrical engineering from the University of Minnesota, Minneapolis, in 1987.

Currently, he is a Chair Professor in the Department of Electrical and Computer Engineering, University of Toronto, Toronto, Ont., Canada, with the title of the Nortel Professor of Emerging Technology. He is the Director of the Nortel Institute at the University of Toronto and is a principal investigator of the Ontario Laser and Lightwave Research Centre. He is also a principal investigator

of the Ontario Centre for Material Research and a key associate of the Information Technology Research Centre. He has authored and co-authored more than 100 refereed papers in physics and engineering journals, and more than 60 refereed conference papers. He has been granted ten patents on electronic and photonic devices. His current research interests include semiconductor physics, nanostructures, quantum electronics, and compound semiconductor device design, modeling and measurements. Currently, he leads a group of 12 researchers and graduate students at the Optoelectronics Laboratory, University of Toronto, and conducts research primarily in the areas of optoelectronics, quantum electronics, nanostructure physics, heterostructure transistors, quantum-well electronics, and photonic devices, as well as large-scale computer simulations. The Optoelectronics Laboratory is sponsored by Nortel and conducts research projects funded by agencies and companies in Canada, U.S., France, and Japan. He is an Editor of the IEEE TRANSACTIONS ON ELECTRON DEVICES.

Prof. Xu was awarded the 1995 Steacie Prize for contributions to fundamental and applied quantum electronics, a 1995 Conference Board Canada-NSERC Award for "Best Practices in University-Industry R&D" (Honorable Mention), and the 1996 FCCP Award of Merit for outstanding contributions in science and technology. One of his students received the NSERC Doctoral Thesis Prize (Engineering), another was given "The Best Student Paper Award LEOS '94," and a third was awarded the Centennial Thesis Prize from the University of Toronto. He is a member of the IEEE Electron Device Society Meetings Committee and ex-officio of the IEEE Electron Device Society Administration Committee.